

POINTS: IMPROVING YOUR VISION-LANGUAGE MODEL WITH AFFORDABLE STRATEGIES

Anonymous authors

Paper under double-blind review

ABSTRACT

In recent years, vision-language models have achieved significant advancements, excelling in tasks once deemed challenging, such as optical character recognition and geometric problem-solving. Despite these impressive achievements, several critical issues remain unaddressed: 1) Proprietary models rarely disclose detailed information about their architectures. In contrast, while open-source models provide visibility into their training strategies, detailed ablations of these strategies are highly anticipated. 2) Pre-training data is currently under-explored in open-source works, with most efforts empirically adding datasets from diverse sources, making the entire process elusive and cumbersome. 3) During the fine-tuning stage, the focus is often on adding and ablating more datasets, which frequently leads to diminishing returns. Therefore, refining data schemes is essential for further enhancing model performance. To address these issues, we propose the following contributions in this paper: 1) We trained a robust baseline model, leveraging the latest technological advancements in vision-language models. Building upon existing advancements, we introduced effective improvements and conducted comprehensive ablation and validation for each technique incorporated into this strong baseline. 2) Inspired by recent work on large language models, we propose filtering pre-training data using perplexity, selecting the data with the lowest perplexity as the training set. This approach allowed us to train on a curated 1M dataset, resulting in highly competitive performance. 3) During the visual instruction tuning stage, we experimented with model soup on different datasets when further introducing more datasets into the training set brought marginal improvements. Integrating these innovations, we obtained a model with 9B parameters, performing competitively with a series of existing state-of-the-art models. Additionally, these strategies we propose are efficient and relatively lightweight, allowing the community to adopt them easily for their models.

1 INTRODUCTION

Advancements in large language models (LLMs; Chowdhery et al. 2023, Jiang et al. 2023, OpenAI 2022, Yang et al. 2024, Dubey et al. 2024) have significantly enhanced the capabilities of vision-language large models (Fu et al. 2023, Liu et al. 2023b, OpenAI 2023, Dong et al. 2024a, Zhu et al. 2023), enabling more sophisticated analyses of textual and visual information. Prominent closed-source model paradigms such as GPT-4 (OpenAI, 2023), Gemini Pro 1.5 (Fu et al., 2023), and Claude 3 (Anthropic, 2024) have achieved remarkable success in expanding LLMs into the realm of vision-language models. Concurrently, open-source vision-language large models are also advancing rapidly, with numerous notable contributions emerging in the field (Liu et al., 2024b; Chen et al., 2024d).

Historically, LLaVA (Liu et al., 2024b) has served as a common baseline. However, recent advancements have rendered its performance suboptimal. Thus, there is a need to establish a stronger baseline for further exploration. In this work, we enhance the vanilla LLaVA architecture by refining the pre-training dataset. Inspired by CapFusion (Yu et al., 2024), we merge the original captions with world knowledge and generated captions that exhibit good grammatical structure. For visual instruction tuning datasets, we introduce Individual Select (Liu et al., 2024c) to curate effective instruction tuning datasets. Regarding model architecture, we first incorporate Dynamic High Resolution to help the model capture fine-grained details. To address image distortion issues inherent

054 in Dynamic High Resolution, we propose a novel image splitting strategy called Consistent Aspect
055 Ratio Dynamic High Resolution (CATTY), which maintains a consistent image ratio. Additionally,
056 inspired by Vary (Wei et al., 2023), we merge features from a vision encoder trained separately with
057 text-rich data with those from the original vision encoder, significantly boosting the model’s optical
058 character recognition (OCR) capabilities. Unlike most existing works (Li et al., 2024a; Chen et al.,
059 2024d), we extensively ablate each newly introduced component in the strong baseline to verify
060 their individual benefits.

061 Recent works seldom explore the optimization of pre-training datasets. Most studies (Chen et al.,
062 2024d; Yao et al., 2024; Bai et al., 2023b) tend to empirically combine samples from various large-
063 scale datasets (Schuhmann et al., 2022; Byeon et al., 2022), often leading to inefficient and com-
064 putationally expensive pre-training processes. In the domain of large language models, some re-
065 search leverages perplexity to filter pre-training datasets. Inspired by this approach, we filter our
066 pre-training dataset by selecting the top samples with the lowest perplexity values. This filtering
067 process yields a subset of 1 million data samples, on which we subsequently pre-train our model.
068 Experimental results demonstrate that the model trained on this filtered subset outperforms a model
069 trained on a dataset five times larger.

070 In the visual instruction tuning stage, most existing works (Liu et al., 2024c; Li et al., 2024a; Chen
071 et al., 2024d) focus on collecting large quantities of datasets and performing ablation studies to
072 select the most effective ones. However, this approach often reaches a plateau, where introducing
073 additional datasets yields only marginal or even degraded performance. Previous research on model
074 soup has demonstrated the benefits of merging weights from different models fine-tuned with various
075 hyper-parameters. In this work, we propose using model soup to merge weights from models fine-
076 tuned with different datasets to further improve performance when dataset selection no longer brings
077 significant improvement. Compared to conducting model soup on models fine-tuned with different
078 hyper-parameters, *e.g.* learning rate, the improvement with model soup on models fine-tuned with
079 different datasets is much more prominent. Following this line of work, we further experiment with
080 different model soup strategies and find that greedy model soup is the most effective.

081 By integrating the aforementioned innovations, we have developed a model called **POINTS**. Our
082 contributions are threefold:

- 083 • We propose a strong baseline that integrates the latest advancements in vision-language models
084 and thoroughly verify the effectiveness of each component.
- 085 • We introduce the use of perplexity to filter the pre-training dataset and conduct a detailed investi-
086 gation of data distribution across different perplexity intervals.
- 087 • We employ model soup to merge models fine-tuned with different datasets, thereby enhancing
088 model performance when further dataset selection yields only marginal improvements.

091 2 RELATED WORKS

092
093
094 **Multimodal Large Language Models** The rapid advancement of large language models (LLMs;
095 Dubey et al. 2024, Team et al. 2023, Achiam et al. 2023, Yang et al. 2024, Su et al. 2022) has laid
096 the groundwork for the emergence of multimodal large language models (MLLMs; Li et al. 2024a,
097 Liu et al. 2024b, Liu et al. 2024a, Bai et al. 2023a, Qiao et al. 2024), which aim to integrate visual
098 understanding with language reasoning and multimodal perception and comprehension. Prominent
099 models such as GPT-4v (Achiam et al., 2023) and Gemini-1.5-Pro (Team et al., 2023), developed
100 by major corporations, have spearheaded the MLLM era, utilizing proprietary training data and
101 undisclosed training methodologies. Meanwhile, open-source models have been striving to keep
102 pace. For instance, LLaVA-Next (Liu et al., 2024a) and InternVL-1.5 (Chen et al., 2024d) introduce
103 dynamic high-resolution techniques by dividing a large image into multiple smaller segments with
104 ratio-inconsistent resizing. MiniCPM-V (Yao et al., 2024) employs a specialized vision encoder to
105 generate non-square image patches. Additionally, models like Vary (Wei et al., 2023), SPHINX (Lin
106 et al., 2023), Cambrian-1 (Tong et al., 2024), and Mini-Gemini (Li et al., 2023a) propose dual vision
107 encoders to enhance visual capabilities. Furthermore, the significant progress in multimodal model
evaluation (Liu et al., 2023c; Chen et al., 2024c; Fang et al., 2024) has also contributed to the rapid
improvement of large vision-language models. In this work, we introduce POINT, a model trained

exclusively with fully open-source datasets during both the pre-training and supervised fine-tuning (SFT) stages, demonstrating promising results on extensive benchmarks.

Visual Instruction Tuning The selection of training data for multimodal models is of paramount importance (Laurençon et al., 2024; Tong et al., 2024), and most improvements in existing works stem from detailed ablation of instruction tuning datasets (Li et al., 2024a; Liu et al., 2024b; Chen et al., 2024d). The commonly used approach to select the most effective datasets involves iteratively adding each dataset to the pool; if it brings improvement, we keep it, otherwise, we drop it. However, this approach may eventually plateau, as further additions might only yield marginal improvements. Previous work He et al. (2024) has shown the benefits of weight merging, but their experimental results are relatively preliminary. To further enhance performance, we systematically propose employing model soup (Wortsman et al., 2022) on different models fine-tuned with various visual instruction tuning datasets. This method involves merging the model weights after visual instruction tuning on diverse datasets, resulting in notable performance improvements.

3 METHODS

This section is divided into three parts: i) In subsection 3.1, we integrate various techniques from previous methods (Liu et al., 2024a; Lin et al., 2023; Wei et al., 2023; Liu et al., 2024c; Chen et al., 2024d) to create a strong baseline for further experiments. Additionally, we propose a novel dynamic resolution splitting method, termed **Consistent Aspect Ratio Dynamic High Resolution (CATTY)** for short, to mitigate the issue of image distortion. ii) In subsection 3.2, we propose using perplexity to filter the pre-training dataset. iii) Finally, in subsection 3.3, we incorporate the concept of model soup (Wortsman et al., 2022) into the instruction tuning stage. We find that this straightforward approach can significantly improve the model’s performance, especially when further data selection only brings marginal or even degraded performance.

3.1 A STRONG BASELINE

In this section, we integrate the recent advancements from existing works to create a strong baseline, containing **Dynamic High Resolution** from InternVL1.5 (Chen et al., 2024d), **CapFusion** from (Yu et al., 2024), **Dual Vision Encoder** from Vary (Wei et al., 2023) and SPHINX (Lin et al., 2023), **Individual Select** from (Liu et al., 2024c). Following LLaVA (Liu et al., 2024b), POINTS mainly contains three parts: vision encoder, projector and the large language model. By integrating all these practices from previous works, we obtain the model structure and pipeline in Figure 1.

Dynamic High Resolution It has been verified that feeding high-resolution images to vision-language models is beneficial for capturing fine-grained details and reducing hallucinations (Liu et al., 2023b). To enable vision encoder with fixed input resolutions to accommodate dynamic image resolutions, Dynamic High Resolution in LLaVA-Next (Liu et al., 2024a) and InternVL-1.5 (Chen et al., 2024d) splits high-resolution images into several tiles of the same resolution, which the original vision encoder can process. The concrete steps are as follows: i) First, the maximum number of tiles an image can be split into is predefined (set to 8 in our experiments). ii) Based on the maximum number of tiles, a table is created containing information about the target image before splitting. The key of the table is the aspect ratio, and the value is the width and height of the target image, which can be evenly divided by the resolution of the vision encoder. iii) For each image, the target resolution is fetched from the pre-computed table according to the similarity between aspect ratios. The current image is then resized to the target resolution and split into several tiles of the same resolution.

Consistent Aspect Ratio Dynamic High Resolution (CATTY) Before splitting the image, Dynamic High Resolution in InternVL-1.5 (Chen et al., 2024d) resizes the image to the target resolution. However, this resizing is not proportional to the image’s original aspect ratio, which can cause distortion. This issue has been discussed in previous articles (Yao et al., 2024). Therefore, we propose a splitting method that maintains the image’s aspect ratio, named Consistent Aspect Ratio Dynamic High Resolution (see Figure 2). The first two steps in CATTY are the same as those in InternVL-1.5, and the last step works as follows: Given an image with height H and width W , we obtain the height and width of the referenced image from the pre-computed table, denoted as H^t and W^t , respectively. Then, we resize the image to the target size ($H^t \times W^t$) by:

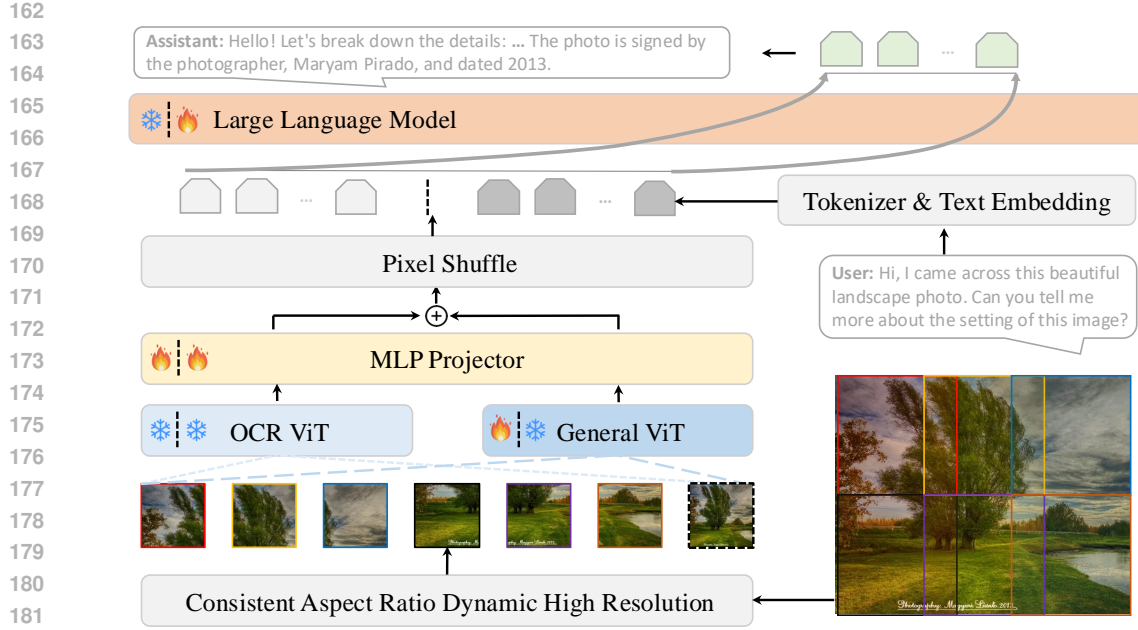


Figure 1: **The architecture of POINTS.** For each module (e.g. OCR ViT, General ViT, MLP Projector, and Large language model), the label to the left of the dash line indicates the status during pre-training, while the label to the right indicates the status during the instruction tuning stage.

$$\begin{aligned}
 \text{ratio} &= \min(H, W) / \min(H^t, W^t) \\
 H^t &= \text{ratio} \times H \\
 W^t &= \text{ratio} \times W
 \end{aligned} \tag{1}$$

Given the input resolution of a vision encoder, $H^v \times W^v$, the target image should be divided into $\frac{H^t}{H^v} \times \frac{W^t}{W^v}$ tiles. Next, we split the target image, $H^t \times W^t$, using a sliding window with strides (S^h, S^w) across the height and width, respectively. The strides (S^h, S^w) are computed as follows:

$$\begin{aligned}
 S^h &= (H^t - H^v) / (H^t / H^v - 1) \\
 S^w &= (W^t - W^v) / (W^t / W^v - 1)
 \end{aligned} \tag{2}$$

In Equation 2, S^h is set to 0 if $H^t / H^v = 1$, and similarly for S^w . This approach allows us to divide a high-resolution image into several tiles without introducing any distortion. There is one exception: if the aspect ratio of the original image is larger than 8, we resize it to an aspect ratio of 1:8 by default. Alongside the tiles obtained using CATTY, we also include a thumbnail of the global view of the image to capture the overall context. This thumbnail is resized to match the input resolution of the vision encoder. Before feeding the features output by the vision encoder into the large language model, we employ the *pixel shuffle* technique with a down-sampling factor of 0.25, as described in InternLM-XComposer2-4KHD (Dong et al., 2024b), to reduce the sequence length of the image features for improved efficiency.

CapFusion The original captions in existing pre-training datasets are often noisy and structurally flawed, making them sub-optimal for model training. To address this, synthetic captions, such as those in LAION-COCO and BLIP-LAION (Li et al., 2022), generated by image captioning models, have been proposed. However, the simplistic syntactic and semantic structures in synthetic captions may contribute to issues like *Scalability Deficiency and World Knowledge Loss* (Yu et al., 2024). CapFusion strikes a balance between these two types of captions by utilizing a large language model to organically integrate raw and synthetic captions. This approach extracts real-world knowledge from the structurally flawed raw captions while merging it with the structured but syntactically simplified synthetic captions. Following the CapFusion methodology, we use InternLM-XComposer2

216
217
218
219
220
221
222
223
224
225
226
227
228
229
230
231
232
233
234
235
236
237
238
239
240
241
242
243
244
245
246
247
248
249
250
251
252
253
254
255
256
257
258
259
260
261
262
263
264
265
266
267
268
269

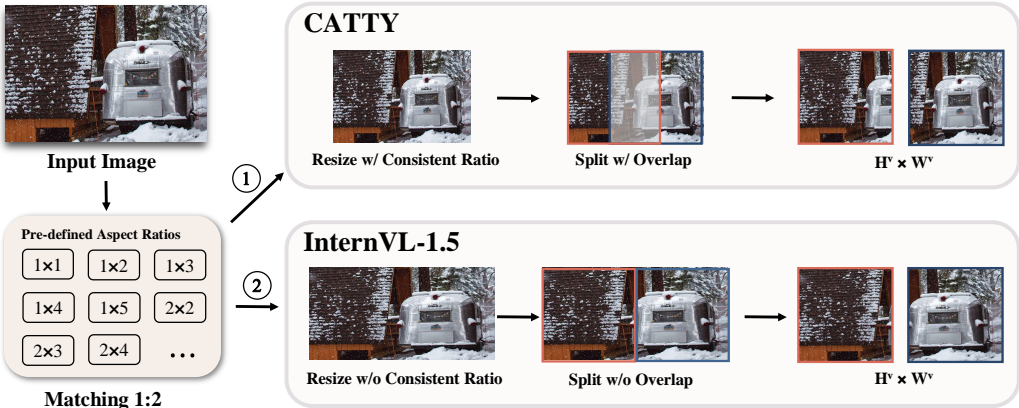


Figure 2: Comparison between dynamic high resolution in InternVL-1.5 and Consistent Aspect Ratio Dynamic High Resolution (CATTY) proposed by us.

(Dong et al., 2024a) to generate captions for images and InternLM2 (Cai et al., 2024) to integrate the original raw and synthetic captions. The prompts to generate image captions and merge captions are in the Appendix.

Dual Vision Encoder Several previous works, such as SPHINX (Lin et al., 2023) and Cambrian-1 (Tong et al., 2024), have demonstrated that different vision encoders exhibit distinct advantages across various domains. Combining features from multiple encoders can lead to improved and more robust performance. Unlike the perception and reasoning required for natural images, text-intensive images demand different capabilities from vision-language models (Wei et al., 2023). To enhance optical character recognition (OCR) capabilities, we train a separate vision encoder, referred to as the OCR ViT, to extract textual features from images, following the methodology of Vary (Wei et al., 2023). Unlike Vary, we do not construct training samples, such as charts, ourselves; instead, we utilize OCR results (extracted using PaddleOCR in our case) for pre-training. Additionally, we include natural captions in the pre-training dataset for the OCR vision encoder. More details about the composition of the pre-training datasets for the OCR vision encoder will be discussed in the following section. We merge the features from the general vision encoder (General ViT) and the OCR vision encoder using a weighted average before feeding them into the large language model.

Individual Select Individual Select, as proposed by Liu et al. (2024c), aims to identify the most effective instruction tuning datasets. Building on this approach, we adopt the dataset composition from Liu et al. (2024c) as our candidate pool and incorporate additional datasets used in DeepSeek-VL (Lu et al., 2024a), Cambrian-1 (Tong et al., 2024), and Cauldron (Laurençon et al., 2024b). Ultimately, we integrate 16 more datasets into those identified by Liu et al. (2024c) (further details are provided in Appendix). To enhance the diversity of prompts, given the homogeneity in the style of prompts within academic datasets, we employ GPT-4o to generate question-answer pairs in line with previous works (Lu et al., 2024a; Chen et al., 2024d) (the prompt to generate question-answer pairs will be provided in the Appendix). The images for these pairs are randomly selected from LAION-5B (Schuhmann et al., 2022). We refer to the final composition of visual instruction tuning datasets as the **Base Set**.

3.2 PRE-TRAIN DATA SELECTION

In the context of large language models, perplexity has long been employed as a metric to assess the quality of pre-trained datasets (Albalak et al., 2024; Marion et al., 2023). Inspired by this approach, we utilize an off-the-shelf vision-language model, P —either the model obtained through the steps outlined in subsection 3.1 or an open-sourced VLM—to further filter out low-quality pre-trained datasets obtained via Capfusion, as described above. For each item, s , in the pre-trained dataset mentioned in subsection 3.1, we compute the perplexity for all text tokens using the following formula:

$$\text{Perplexity}(s) = \exp\left(-\frac{1}{N} \sum_{i=1}^N \log P(w_i | w_1, w_2, \dots, w_{i-1})\right) \quad (3)$$

Let $\{w_1, \dots, w_N\}$ represent the text token sequence for s . We sort all these items in ascending order and select the first 20% for the pre-training stage. Upon closer examination of the first and last 20% of items, we observe that the distinguishing factor is not the quality of the data, which contrasts with observations in large language models. The last 20% of items often contain obscure world knowledge, such as game version numbers and computer factory serial numbers. This type of world knowledge is extremely rare and contains very little information, making it less beneficial for the model’s learning. In the Appendix, we provide some examples randomly sampled from the first and last 20% of items.

3.3 INSTRUCTION DATA SELECTION WITH MODEL SOUP

Visual instruction tuning data is crucial for the superior performance of existing vision-language models (Chen et al., 2024d; Dong et al., 2024a; Liu et al., 2024b). However, most existing works focus on selecting more effective datasets by iterative ablation. In many cases, this approach reaches a plateau, where further data selection can only bring marginal improvements or even degrade performance. In this section, we systematically introduce the benefits of using model soup to integrate the advantages of models fine-tuned with different instruction tuning datasets after data selection meets a bottleneck. The philosophy behind model soup is as follows: given a pre-trained model, fine-tuning the model with different hyper-parameters, h_1, \dots, h_k , results in several fine-tuned models converging to different local optima, denoted as $f(\theta_1, h_1), \dots, f(\theta_k, h_k)$. These hyper-parameters include learning rate, data augmentation, initialization seed, etc. By interpolating the weights of these fine-tuned models, we can always obtain a stronger model, $f(\theta_s, h_s)$. Given the pre-trained model obtained through the methods discussed above, a base instruction tuning dataset D , and a series of visual instruction tuning datasets d_1, \dots, d_k to be selected, we can obtain a stronger model using the following steps:

- For each dataset $d_i \in \{d_1, \dots, d_k\}$, we add it to the base instruction tuning dataset, D , to obtain an augmented dataset, D_i^* .
- We train k models using each augmented from $\{D_1^*, \dots, D_k^*\}$ concurrently, and obtain $\{f(D_1^*; \theta_1), \dots, f(D_k^*; \theta_k)\}$.
- We select p models from $\{f(D_1^*; \theta_1), \dots, f(D_k^*; \theta_k)\}$, and merge the weights from all these selected models to obtain a stronger model.

For the third step above, we choose several methods to select the best composition of fine-tuned models to obtain a final model with superior performance, namely, *Maximum Soup*, *Average Soup*, and *Greedy Soup*.

Maximum Soup Given an evaluation score, Acc , we can obtain a strong model, $f(\theta_s)$, using the following formula:

$$\begin{aligned} \{\theta_i\}_{\text{len}(\{\theta_i\})=p} &= \text{Arg}_{(\theta_i)}(\text{Top}_p(\{\text{Acc}(f(D_1^*; \theta_1)), \dots, \text{Acc}(f(D_k^*; \theta_k))\})) \\ f(\theta_s) &= f\left(\frac{1}{p} \sum_{i=1}^p \theta_i\right) \end{aligned} \quad (4)$$

Average Soup By taking the average of weights from all fine-tuned models, we can obtain a stronger model, $f(\theta_s)$:

$$f(\theta_s) = f\left(\frac{1}{k} \sum_{i=1}^k \theta_i\right) \quad (5)$$

Greedy Soup We start by sorting the fine-tuned models in descending order based on their evaluation scores. Next, we iterate through these sorted models. For each model, we compute the average

of its weights with those of all models currently in the model pool. If the evaluation score improves, the model is added to the pool. Finally, we average the weights of all models in the pool to obtain a stronger model, denoted as $f(\theta_s)$. The table below outlines the detailed pipeline of Greedy Soup.

Algorithm 1 Greedy Soup for Visual Instruction Tuning Datasets

```

1: INPUT:  $k$  fine-tuned models with different datasets,  $\{f(D_i^*; \theta_i)\}$ 
2: INPUT: the evaluation score, Acc
3: INPUT: model pool,  $P \leftarrow \{\}$ 
4: for  $i = 1$  to  $k$  do
5:   if  $\text{Acc}(f(\text{average}(P, \theta_i))) \geq \text{Acc}(f(\text{average}(P)))$  then
6:      $P \leftarrow P \cup \theta_i$ 
7:   end if
8: end for
9: Return  $\text{average}(P)$ 

```

4 EXPERIMENTS

This section is divided into five subsections: (i) evaluation setup, (ii) pre-training and instruction-tuning datasets used to train the strong baseline (iii) details about the training setup for the OCR ViT pre-training, the vision-language pre-training, and the visual instruction tuning stages, (iv) ablation studies and analyses of each component used to build our final model, and (v) comparison with other works on extensive benchmarks.

4.1 EVALUATION SETUP

Before embarking on our exploration, we sought a robust evaluation metric to comprehensively assess the various capabilities of our model. This is where OpenCompass (Contributors, 2023) proves helpful. OpenCompass proposes eight benchmarks to balance the evaluation of a model from different perspectives. These benchmarks include MMBench (Liu et al., 2023c) and MMStar (Chen et al., 2024b) for diagnosing general abilities, MMMU (Yue et al., 2024) for testing STEM-related abilities, HallusionBench (Liu et al., 2023a) for model hallucination, MathVista (Lu et al., 2023) for math-related abilities, AI2D (Kembhavi et al., 2016) for chart-related abilities, OCRBench (Liu et al., 2023d) for OCR capabilities, and MMVet (Yu et al., 2023b) for subjective evaluation. By averaging the metrics from these benchmarks, OpenCompass derives a score that represents the comprehensive ability of a model. Additionally, it offers a useful tool, VLMEvalKit (Duan et al., 2024), for one-click evaluation. Therefore, unless otherwise specified, we will use these eight benchmarks for our ablation study, with the exception of MMBench, for which we will use the *dev-en* split.

4.2 DATA SETUP

Pre-train Dataset To train the OCR ViT, we randomly selected 20 million data points from LAION-5B-en (Schuhmann et al., 2022), LAION-5B-cn (Schuhmann et al., 2022), WuKong (Gu et al., 2022), and Zero (Gu et al., 2022). We then used PaddleOCR to extract text from the images, replacing the original captions to form new image-caption pairs for pre-training. Following Vary (Wei et al., 2023), we also included 10 million original data samples from LAION-5B, where the captions are the original ones crawled from the Internet. However, we did not adopt the cumbersome pipeline of constructing a new dataset for OCR enhancement, such as crawling PDF files and converting them to images for training (Bai et al., 2023b), as we found our existing pipeline already performs well on OCR-related tasks. For the vision-language pre-training in constructing the strong baseline, we used CapFusion to construct 20 million data points (note that these data do not overlap with those used in OCR ViT pre-training) from LAION-5B. From this set, we selected 5 million data points, as we found this setting works best, similar to the observation in Liu et al. (2024c). Based on the 5 million data, we further selected a 1 million dataset for the final vision-language alignment by choosing the top 20% of data with the lowest perplexity value.

Visual Instruction Tuning Dataset Based on the datasets identified by Liu et al. (2024c), we further employ **Individual Select** to choose additional datasets from those proposed in (Lu et al., 2024a), (Tong et al., 2024), and (Laurençon et al., 2024b). The final composition of datasets, referred to as the **Base Set**, used to construct the robust baseline is presented in Appendix.

4.3 TRAINING SETUP

Pre-training Setup for OCR ViT The pre-training framework follows the standard LLaVA-style architecture (Liu et al., 2023b), comprising a vision encoder, a two-layer MLP, and a large language model. The vision encoder is initialized from OpenAI’s CLIP-ViT-Large-336, while the large language model is initialized from Yi-1.5-9B-Chat (Young et al., 2024). Throughout the pre-training stage, the large language model remains frozen, whereas the vision encoder and MLP are trainable. The learning rates for the vision encoder and MLP are set to 2×10^{-4} and 2×10^{-5} , respectively, with a warm-up schedule during the first 3% of steps, followed by a cosine decay schedule for the remaining steps.

Setup for the Vision-language Pre-training Stage The General ViT, depicted in Figure 1, is initialized from OpenAI’s CLIP-ViT-Large-336, while the OCR ViT is derived from the preceding stage. For the General ViT, only the last three layers are trainable, as this configuration yielded the best results in our experiments. The OCR ViT remains frozen throughout this stage, consistent with the settings used in Vary(Wei et al., 2023). Features from the penultimate layer of both the General and OCR ViT are selected and fed into the projector. The projector itself is a two-layer MLP, which remains tunable during the pre-training stage. The learning rates for the General ViT and the MLP are set to 2×10^{-4} and 2×10^{-5} , respectively. A warm-up schedule is applied during the first 3% of steps, followed by a cosine decay schedule for the remaining steps.

Setup for the Visual Instruction Tuning Stage Both the General ViT and OCR ViT remain frozen throughout the entire stage. The learning rates for the projector and the large language model are both set to 2×10^{-5} . A warm-up schedule is applied during the first 3% of steps, followed by a cosine decay schedule for the remaining steps.

4.4 ABLATION STUDY AND ANALYSIS

Each Component to Build the Strong Baseline As shown in Table 1, each component introduced in subsection 3.1 contributes to steady improvements. These enhancements are significant; for instance, after introducing Dynamic High Resolution to split the input image, we observe substantial improvements in OCR-related tasks, such as OCRBench, with performance increasing from 49.6% to 55.6%. Additionally, the use of high-resolution images with Dynamic High Resolution helps reduce hallucination, primarily due to the increased detail in the high-resolution images. Furthermore, replacing the original Dynamic High Resolution with CATTY results in notable improvements across various benchmarks, with OCR-related benchmarks showing greater gains than others. This is likely because image distortion has a more pronounced negative impact on text within images. Compared to general visual feature extraction, the ability to extract text features from images is limited for CLIP-ViT(Radford et al., 2021), as it was trained on a large quantity of general image-text pairs. Consequently, we observe substantial improvements on OCRBench after integrating features from an additional ViT, post-trained on text-rich images. Among the 5 strategies, incorporating more visual instruction tuning datasets by Individual Select yields the most significant improvements. This observation aligns with existing works(Chen et al., 2024d; Li et al., 2024a; Tong et al., 2024), underscoring the importance of selecting effective datasets during the visual instruction tuning stage.

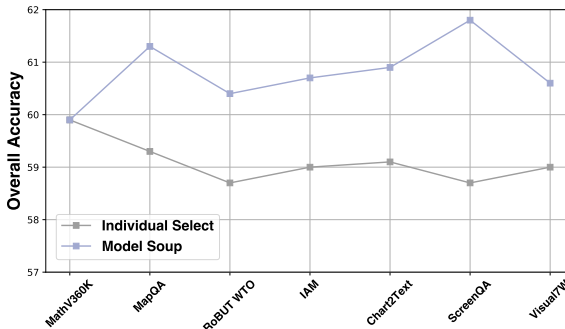


Figure 3: **The superiority of Model Soup.** When adding additional instruction tuning datasets no longer yields benefits (Individual Select), Model Soup can significantly enhance performance.

CF	DHR	CATTY	DVE	IS	MMB	MV	HB	OCR	AI2D	MMVet	MMStar	MMMU	Overall
					72.1	43.8	35.7	48.9	73.2	40.0	51.5	36.2	50.2
✓					74.8	44.8	35.5	49.6	74.5	41.2	51.8	36.4	51.1
✓	✓				75.1	45.1	38.0	55.6	75.0	42.2	52.6	37.5	52.6
✓		✓			75.9	45.7	39.1	56.9	75.8	43.1	52.4	37.9	53.4
✓		✓	✓		77.3	49.2	42.3	60.3	76.0	44.5	54.3	40.1	55.5
✓		✓	✓	✓	80.1	57.4	44.2	69.2	76.4	47.2	54.5	43.3	59.0

Table 1: **Ablation about each component to build the strong baseline.** CF: CapFusion(Yu et al., 2024), DHR: Dynamic high resolution(Chen et al., 2024d), CATTY: Consistent aspect ratio dynamic high resolution proposed by us, DEV: Dual vision encoder(Wei et al., 2023), IS: Individual select(Liu et al., 2024c). MMB: the *dev-en* split of MMBench(Liu et al., 2023c), MV: MathVista(Lu et al., 2023), HB: HallusionBench(Liu et al., 2023a), OCR: OCRBench(Liu et al., 2023d), Overall: the average of scores on the first 8 benchmarks.

#num	perplexity	Overall	DVE	SVE	OCR	Overall	lr	ds	Model Soup	Overall
5M		59.0	✓		69.2	59.0			baseline	59.0
20M		58.8		✓	67.3	57.2	✓		Greedy Soup	59.2
1M	✓	59.6						✓	Maximum Soup	61.0
								✓	Average Soup	61.2
								✓	Greedy Soup	61.8

Table 2: The first two rows compare the use of different data quantities during the pre-training stage. The third row represents a subset of the 5M dataset from the first row, filtered by perplexity.

Table 3: **DVE**: Dual Vision Encode. **SVE**: Single Vision Encoder, incorporating the OCR dataset used to train the OCR ViT into the dataset for the vision-language pre-training stage.

Table 4: Comparison of different model soup strategies over visual instruction tuning datasets. **lr**: model soup on models fine-tuned with different learning rates. **ds**: model soup on models fine-tuned with different datasets.

Pre-train Dataset As shown in Table 2, scaling up the dataset size (constructed by CapFusion) from 5M to 20M results in downgraded performance, similar to the observations in Liu et al. (2024c). Additionally, some works also achieve promising performance using relative small pre-training datasets instead of a huge number of datasets during the pre-training stage (Li et al., 2024a; Liu et al., 2024a). We believe the possible reasons are: i) The vision encoder of most existing vision-language models is initialized from a pre-trained model that has already been trained on a large quantity of image-text pairs. It is highly likely that most of the data used in the vision-language pre-training stage has already been seen by the vision encoder, thus bringing only marginal or even negative impact when scaling up the size of the vision-language pre-training dataset. ii) The pre-training datasets are quite homogeneous for existing large-scale web-crawled datasets, *e.g.*, LAION-5B and COYO-700M (Byeon et al., 2022). We plot the distribution of the main entity for each image of a subset extracted from LAION-5B in the Appendix and find that this distribution is long-tailed and constrained to a few objects, *e.g.*, person. Thus, indiscriminately pre-training the model on such datasets can only bring limited benefits. As shown in the third row, we can improve performance by pre-training the model on merely 1M data, coming from the top 20% of the 5M data in the first row, which has the lowest perplexity. This result shows that excessively exposing the model to obscure and scarce knowledge during the transition is detrimental to its learning. Furthermore, compared to fusing features from a separate OCR-enhanced vision encoder, introducing a large OCR dataset has two obvious drawbacks: i) During the pre-training stage, the model has to align both the general features and OCR-related features, which may result in conflicts (Wei et al., 2023). ii) Since the size of the dataset used in vision-language pre-training is relatively small, a large OCR dataset may overwhelm the learning process, which is not helpful for learning other kinds of knowledge. Thus, introducing features from another OCR ViT can yield superior performance in Table 3.

Improve the Performance with Model Soup on Different Datasets. As described in previous sections, increasingly adding more instruction tuning datasets often reaches a plateau where further increasing the number of datasets yields minimal improvement. However, by incorporating model soup across different datasets, we observe substantial enhancements, as shown in Table 4, with the overall score increasing from 59.0 to 61.8. We also compare the benefits of various model soup strategies. Among them, greedy soup achieves the best performance, outperforming maximum soup

Methods	MMB	MV	HB	OCR	AI2D	MMVet	MMStar	MMMU	SCI	MME	RWQ	Wild
<i>Proprietary models</i>												
GPT-4o-0513	-	61.3	55.0	73.6	84.6	69.1	63.9	69.2	90.7	2310.3	75.4	102.0
Claude3.5-Sonnet	-	61.6	49.9	78.8	80.2	66.0	62.2	65.9	88.9	1920.0	60.1	81.0
Gemini-1.5-Pro	-	57.7	45.6	75.4	79.1	64.0	59.1	60.6	85.7	2110.6	64.1	95.3
<i>Open-source models</i>												
Cambrian-34B	81.4	50.3	41.6	59.1	79.5	53.2	54.2	50.4	85.6	2049.9	67.1	82.0
Ovis1.5-LLaMA3-8B	-	63.0	45.0	74.4	82.5	50.9	57.3	48.3	88.8	1948.5	64.2	79.9
Idefics3-LLaMA3-8B	-	58.4	43.7	55.0	76.5	41.7	55.0	46.6	91.3	1937.4	62.6	66.3
InternVL2-8B	-	58.3	45.0	79.4	83.6	54.3	61.5	51.2	97.1	2215.1	64.2	73.3
IXC-2.5	-	63.7	43.1	68.6	81.6	49.3	59.9	42.9	96.6	2233.1	67.8	70.2
OneVision	80.8	62.3	31.6	62.2	82.4	51.9	61.9	47.9	95.4	1993.6	69.9	81.0
<i>Ours</i>												
POINTS-9B	83.2	60.7	48.0	70.6	78.5	50.0	56.4	46.9	92.9	2017.8	65.9	69.3

Table 5: **Comparison between different methods.** MMB: the *dev-en* split of MMBench(Liu et al., 2023c), MV: MathVista(Lu et al., 2023), HB: HallusionBench(Liu et al., 2023a), OCR: OCRBench(Liu et al., 2023d), SCI: ScienceQA(Lu et al., 2022a), MME: MME(Yin et al., 2023), RWQ: RealWorldQA, Wild: LLaVA-Wild(Liu et al., 2024b). Cambrian-34: Cambrian-34B(Tong et al., 2024), Ovis1.5-LLaMA3-8B: Ovis1.5(Lu et al., 2024b), IXC-2.5: InternLM-XComposer-2.5(Zhang et al., 2024), OneVision: LLaVA-OneVision(Li et al., 2024a), Idefics3-LLaMA3-8B: IDEFICS3 (Laurençon et al., 2024a). The language model POINTS-9B uses is Yi-1.5-9B (Young et al., 2024). Results are obtained from the leaderboard of OpenCompass, except for MMBench. POINTS-7B uses is Qwen-2.5-7B (Team, 2024).

and average soup by 0.8 and 0.6 points, respectively. Unless otherwise specified, we will use greedy soup by default in subsequent experiments. Additionally, we include the results of conducting model soup over different hyperparameters, *e.g.* different learning rates. As shown, model soup over hyperparameters brings only marginal improvement. Furthermore, we verify in the Appendix that model soup consistently improves performance regardless of the **Base Set** used.

4.5 COMPARISON WITH OTHER WORKS

In addition to the 8 benchmarks used in the ablation studies above, we further include ScienceQA (Lu et al., 2022a), MME (Yin et al., 2023), LLaVA-Wild (Liu et al., 2024b), and ReadWorldQA to compare the performance of different models. The following table shows the performance of these models. As shown in Table 5, POINTS achieves performance comparable to existing state-of-the-art models of similar size and even surpasses models with much larger sizes, such as Cambrian-34B. Additionally, compared to the models listed in the table, POINTS uses a much smaller pre-training dataset (*e.g.*, 1M), fewer visual instruction tuning datasets, and all the datasets we used are publicly available. This makes it more affordable for the community to adopt the strategies proposed in this paper. Furthermore, each aspect of POINTS is clearly presented and thoroughly analyzed, making the effectiveness of each strategy employed in our model evident.

5 CONCLUSION

Vision-language models have achieved significant progress in recent years. Following this trend (Chen et al., 2024d; Li et al., 2024a; Liu et al., 2024b; Zhang et al., 2024; Tong et al., 2024), we first establish a strong baseline by integrating various advancements proposed in recent works (Liu et al., 2024a; Yu et al., 2024; Wei et al., 2023; Liu et al., 2024c) for further experiments. Additionally, we delve into the intricate details of these advancements and propose effective refinements, such as the Consistent Aspect Ratio Dynamic High Resolution. We also conduct extensive experiments to verify the effectiveness of each component in constructing the strong baseline. Secondly, we propose using perplexity to filter the pre-training dataset, retaining only the top 20% of data with the smallest perplexity values during the pre-training stage. This filtering method also brings significant improvements. Model Soup (Wortsman et al., 2022) has shown promising potential to further enhance performance by averaging the weights of fine-tuned models with different hyperparameters. However, we find that conducting model soup over different dataset settings can yield even more substantial improvements.

REFERENCES

- 540
541
542 Josh Achiam, Steven Adler, Sandhini Agarwal, Lama Ahmad, Ilge Akkaya, Florencia Leoni Ale-
543 man, Diogo Almeida, Janko Altenschmidt, Sam Altman, Shyamal Anadkat, et al. Gpt-4 technical
544 report. *arXiv preprint arXiv:2303.08774*, 2023.
- 545 Alon Albalak, Yanai Elazar, Sang Michael Xie, Shayne Longpre, Nathan Lambert, Xinyi Wang,
546 Niklas Muennighoff, Bairu Hou, Liangming Pan, Haewon Jeong, et al. A survey on data selection
547 for language models. *arXiv preprint arXiv:2402.16827*, 2024.
- 548 Anthropic. Claude 3 haiku: Our fastest model yet, 2024. URL <https://www.anthropic.com/news/claude-3-haiku>.
549
550
- 551 Jinze Bai, Shuai Bai, Shusheng Yang, Shijie Wang, Sinan Tan, Peng Wang, Junyang Lin, Chang
552 Zhou, and Jingren Zhou. Qwen-vl: A frontier large vision-language model with versatile abilities.
553 *arXiv preprint arXiv:2308.12966*, 2023a.
- 554 Jinze Bai, Shuai Bai, Shusheng Yang, Shijie Wang, Sinan Tan, Peng Wang, Junyang Lin, Chang
555 Zhou, and Jingren Zhou. Qwen-vl: A frontier large vision-language model with versatile abilities.
556 *arXiv preprint arXiv:2308.12966*, 2023b.
557
- 558 Ali Furkan Biten, Ruben Tito, Andres Mafra, Lluís Gomez, Marçal Rusinol, Ernest Valveny,
559 CV Jawahar, and Dimosthenis Karatzas. Scene text visual question answering. In *Proceedings of*
560 *the IEEE/CVF international conference on computer vision*, pp. 4291–4301, 2019.
- 561 Minwoo Byeon, Beomhee Park, Haecheon Kim, Sungjun Lee, Woonhyuk Baek, and Saehoon
562 Kim. Coyo-700m: Image-text pair dataset. [https://github.com/kakaobrain/](https://github.com/kakaobrain/coyo-dataset)
563 [coyo-dataset](https://github.com/kakaobrain/coyo-dataset), 2022.
- 564 Zheng Cai, Maosong Cao, Haojiong Chen, Kai Chen, Keyu Chen, Xin Chen, Xun Chen, Zehui
565 Chen, Zhi Chen, Pei Chu, et al. Internlm2 technical report. *arXiv preprint arXiv:2403.17297*,
566 2024.
567
- 568 Jie Cao and Jing Xiao. An augmented benchmark dataset for geometric question answering through
569 dual parallel text encoding. In Nicoletta Calzolari, Chu-Ren Huang, Hansaem Kim, James Puste-
570 jovsky, Leo Wanner, Key-Sun Choi, Pum-Mo Ryu, Hsin-Hsi Chen, Lucia Donatelli, Heng Ji,
571 Sadao Kurohashi, Patrizia Paggio, Nianwen Xue, Seokhwan Kim, Younggyun Hahm, Zhong
572 He, Tony Kyungil Lee, Enrico Santus, Francis Bond, and Seung-Hoon Na (eds.), *Proceedings*
573 *of the 29th International Conference on Computational Linguistics*, pp. 1511–1520, Gyeongju,
574 Republic of Korea, October 2022. International Committee on Computational Linguistics. URL
575 <https://aclanthology.org/2022.coling-1.130>.
- 576 Shuaichen Chang, David Palzer, Jialin Li, Eric Fosler-Lussier, and Ningchuan Xiao. Mapqa: A
577 dataset for question answering on choropleth maps. *arXiv preprint arXiv:2211.08545*, 2022.
- 578 Guiming Hardy Chen, Shunian Chen, Ruifei Zhang, Junying Chen, Xiangbo Wu, Zhiyi Zhang, Zhi-
579 hong Chen, Jianquan Li, Xiang Wan, and Benyou Wang. Allava: Harnessing gpt4v-synthesized
580 data for a lite vision-language model. *arXiv preprint arXiv:2402.11684*, 2024a.
- 581 Lin Chen, Jisong Li, Xiaoyi Dong, Pan Zhang, Conghui He, Jiaqi Wang, Feng Zhao, and Dahua
582 Lin. Sharegpt4v: Improving large multi-modal models with better captions. *arXiv preprint*
583 *arXiv:2311.12793*, 2023.
584
- 585 Lin Chen, Jinsong Li, Xiaoyi Dong, Pan Zhang, Yuhang Zang, Zehui Chen, Haodong Duan, Jiaqi
586 Wang, Yu Qiao, Dahua Lin, et al. Are we on the right way for evaluating large vision-language
587 models? *arXiv preprint arXiv:2403.20330*, 2024b.
- 588 Pengcheng Chen, Jin Ye, Guoan Wang, Yanjun Li, Zhongying Deng, Wei Li, Tianbin Li, Haodong
589 Duan, Ziyang Huang, Yanzhou Su, et al. Gmai-mmbench: A comprehensive multimodal evaluation
590 benchmark towards general medical ai. *arXiv preprint arXiv:2408.03361*, 2024c.
591
- 592 Zhe Chen, Weiyun Wang, Hao Tian, Shenglong Ye, Zhangwei Gao, Erfei Cui, Wenwen Tong,
593 Kongzhi Hu, Jiapeng Luo, Zheng Ma, et al. How far are we to gpt-4v? closing the gap to com-
mercial multimodal models with open-source suites. *arXiv preprint arXiv:2404.16821*, 2024d.

- 594 Aakanksha Chowdhery, Sharan Narang, Jacob Devlin, Maarten Bosma, Gaurav Mishra, Adam
595 Roberts, Paul Barham, Hyung Won Chung, Charles Sutton, Sebastian Gehrmann, et al. Palm:
596 Scaling language modeling with pathways. *Journal of Machine Learning Research*, 24(240):
597 1–113, 2023.
- 598
599 OpenCompass Contributors. Opencompass: A universal evaluation platform for foundation models.
600 <https://github.com/open-compass/opencompass>, 2023.
- 601 Xiaoyi Dong, Pan Zhang, Yuhang Zang, Yuhang Cao, Bin Wang, Linke Ouyang, Xilin Wei,
602 Songyang Zhang, Haodong Duan, Maosong Cao, Wenwei Zhang, Yining Li, Hang Yan, Yang
603 Gao, Xinyue Zhang, Wei Li, Jingwen Li, Kai Chen, Conghui He, Xingcheng Zhang, Yu Qiao,
604 Dahua Lin, and Jiaqi Wang. Internlm-xcomposer2: Mastering free-form text-image composition
605 and comprehension in vision-language large model. *arXiv preprint arXiv:2401.16420*, 2024a.
- 606
607 Xiaoyi Dong, Pan Zhang, Yuhang Zang, Yuhang Cao, Bin Wang, Linke Ouyang, Songyang Zhang,
608 Haodong Duan, Wenwei Zhang, Yining Li, Hang Yan, Yang Gao, Zhe Chen, Xinyue Zhang, Wei
609 Li, Jingwen Li, Wenhai Wang, Kai Chen, Conghui He, Xingcheng Zhang, Jifeng Dai, Yu Qiao,
610 Dahua Lin, and Jiaqi Wang. Internlm-xcomposer2-4khd: A pioneering large vision-language
611 model handling resolutions from 336 pixels to 4k hd. *arXiv preprint arXiv:2404.06512*, 2024b.
- 612 Haodong Duan, Junming Yang, Yuxuan Qiao, Xinyu Fang, Lin Chen, Yuan Liu, Xiaoyi Dong,
613 Yuhang Zang, Pan Zhang, Jiaqi Wang, et al. Vlmevalkit: An open-source toolkit for evaluating
614 large multi-modality models. *arXiv preprint arXiv:2407.11691*, 2024.
- 615
616 Abhimanyu Dubey, Abhinav Jauhri, Abhinav Pandey, Abhishek Kadian, Ahmad Al-Dahle, Aiesha
617 Letman, Akhil Mathur, Alan Schelten, Amy Yang, Angela Fan, et al. The llama 3 herd of models.
618 *arXiv preprint arXiv:2407.21783*, 2024.
- 619 Xinyu Fang, Kangrui Mao, Haodong Duan, Xiangyu Zhao, Yining Li, Dahua Lin, and Kai Chen.
620 Mmbench-video: A long-form multi-shot benchmark for holistic video understanding. *arXiv*
621 *preprint arXiv:2406.14515*, 2024.
- 622
623 Chaoyou Fu, Renrui Zhang, Haojia Lin, Zihan Wang, Timin Gao, Yongdong Luo, Yubo Huang,
624 Zhengye Zhang, Longtian Qiu, Gaoxiang Ye, et al. A challenger to gpt-4v? early explorations of
625 gemini in visual expertise. *arXiv preprint arXiv:2312.12436*, 2023.
- 626
627 Jiayi Gu, Xiaojun Meng, Guansong Lu, Lu Hou, Niu Minzhe, Xiaodan Liang, Lewei Yao, Runhui
628 Huang, Wei Zhang, Xin Jiang, et al. Wukong: A 100 million large-scale chinese cross-modal
629 pre-training benchmark. *Advances in Neural Information Processing Systems*, 35:26418–26431,
2022.
- 630
631 Muyang He, Yexin Liu, Boya Wu, Jianhao Yuan, Yueze Wang, Tiejun Huang, and Bo Zhao. Efficient
632 multimodal learning from data-centric perspective. *arXiv preprint arXiv:2402.11530*, 2024.
- 633
634 Yu-Chung Hsiao, Fedir Zubach, Maria Wang, et al. Screenqa: Large-scale question-answer pairs
over mobile app screenshots. *arXiv preprint arXiv:2209.08199*, 2022.
- 635
636 Albert Q Jiang, Alexandre Sablayrolles, Arthur Mensch, Chris Bamford, Devendra Singh Chaplot,
637 Diego de las Casas, Florian Bressand, Gianna Lengyel, Guillaume Lample, Lucile Saulnier, et al.
638 Mistral 7b. *arXiv preprint arXiv:2310.06825*, 2023.
- 639
640 Kushal Kafle, Brian Price, Scott Cohen, and Christopher Kanan. Dvqa: Understanding data visual-
641 izations via question answering. In *Proceedings of the IEEE conference on computer vision and*
pattern recognition, pp. 5648–5656, 2018.
- 642
643 Aniruddha Kembhavi, Michael Salvato, Eric Kolve, Minjoon Seo, Hannaneh Hajishirzi, and Ali
644 Farhadi. A diagram is worth a dozen images. *ArXiv*, abs/1603.07396, 2016. URL <https://api.semanticscholar.org/CorpusID:2682274>.
- 645
646 Daesik Kim, Seonhoon Kim, and Nojun Kwak. Textbook question answering with multi-
647 modal context graph understanding and self-supervised open-set comprehension. *arXiv preprint*
arXiv:1811.00232, 2018.

- 648 Jianfeng Kuang, Wei Hua, Dingkan Liang, Mingkun Yang, Deqiang Jiang, Bo Ren, and Xiang
649 Bai. Visual information extraction in the wild: practical dataset and end-to-end solution. In
650 *International Conference on Document Analysis and Recognition*, pp. 36–53. Springer, 2023.
- 651 Hugo Laurençon, Andrés Marafioti, Victor Sanh, and Léo Tronchon. Building and bet-
652 ter understanding vision-language models: insights and future directions. *arXiv preprint*
653 *arXiv:2408.12637*, 2024a.
- 654 Hugo Laurençon, Léo Tronchon, Matthieu Cord, and Victor Sanh. What matters when building
655 vision-language models? *arXiv preprint arXiv:2405.02246*, 2024b.
- 656 Hugo Laurençon, Léo Tronchon, Matthieu Cord, and Victor Sanh. What matters when building
657 vision-language models?, 2024. URL <https://arxiv.org/abs/2405.02246>.
- 658 Bo Li, Yuanhan Zhang, Dong Guo, Renrui Zhang, Feng Li, Hao Zhang, Kaichen Zhang, Yanwei
659 Li, Ziwei Liu, and Chunyuan Li. Llava-onevision: Easy visual task transfer. *arXiv preprint*
660 *arXiv:2408.03326*, 2024a.
- 661 Junnan Li, Dongxu Li, Caiming Xiong, and Steven Hoi. Blip: Bootstrapping language-image pre-
662 training for unified vision-language understanding and generation. In *International conference on*
663 *machine learning*, pp. 12888–12900. PMLR, 2022.
- 664 Shen Li, Yanli Zhao, Rohan Varma, Omkar Salpekar, Pieter Noordhuis, Teng Li, Adam Paszke, Jeff
665 Smith, Brian Vaughan, Pritam Damania, et al. Pytorch distributed: Experiences on accelerating
666 data parallel training. *arXiv preprint arXiv:2006.15704*, 2020.
- 667 Yanwei Li, Yuechen Zhang, Chengyao Wang, Zhisheng Zhong, Yixin Chen, Ruihang Chu, Shaoteng
668 Liu, and Jiaya Jia. Mini-gemini: Mining the potential of multi-modality vision language models.
669 *arXiv:2403.18814*, 2023a.
- 670 Yanwei Li, Yuechen Zhang, Chengyao Wang, Zhisheng Zhong, Yixin Chen, Ruihang Chu, Shaoteng
671 Liu, and Jiaya Jia. Mini-gemini: Mining the potential of multi-modality vision language models.
672 *arXiv preprint arXiv:2403.18814*, 2024b.
- 673 Zhuowan Li, Xingrui Wang, Elias Stengel-Eskin, Adam Kortylewski, Wufei Ma, Benjamin
674 Van Durme, and Alan L Yuille. Super-clevr: A virtual benchmark to diagnose domain robust-
675 ness in visual reasoning. In *Proceedings of the IEEE/CVF Conference on Computer Vision and*
676 *Pattern Recognition*, pp. 14963–14973, 2023b.
- 677 Ziyi Lin, Chris Liu, Renrui Zhang, Peng Gao, Longtian Qiu, Han Xiao, Han Qiu, Chen Lin, Wenqi
678 Shao, Keqin Chen, et al. Sphinx: The joint mixing of weights, tasks, and visual embeddings for
679 multi-modal large language models. *arXiv preprint arXiv:2311.07575*, 2023.
- 680 Adam Dahlgren Lindström and Savitha Sam Abraham. Clevr-math: A dataset for compositional
681 language, visual and mathematical reasoning. *arXiv preprint arXiv:2208.05358*, 2022.
- 682 Fuxiao Liu, Tianrui Guan, Zongxia Li, Lichang Chen, Yaser Yacoob, Dinesh Manocha, and Tianyi
683 Zhou. Hallusionbench: You see what you think? or you think what you see? an image-context
684 reasoning benchmark challenging for gpt-4v (ision), llava-1.5, and other multi-modality models.
685 *arXiv preprint arXiv:2310.14566*, 2023a.
- 686 Haotian Liu, Chunyuan Li, Yuheng Li, and Yong Jae Lee. Improved baselines with visual instruction
687 tuning, 2023b.
- 688 Haotian Liu, Chunyuan Li, Yuheng Li, Bo Li, Yuanhan Zhang, Sheng Shen, and Yong Jae Lee.
689 Llava-next: Improved reasoning, ocr, and world knowledge, January 2024a. URL [https://](https://llava-vl.github.io/blog/2024-01-30-llava-next/)
690 llava-vl.github.io/blog/2024-01-30-llava-next/.
- 691 Haotian Liu, Chunyuan Li, Qingyang Wu, and Yong Jae Lee. Visual instruction tuning. *Advances*
692 *in neural information processing systems*, 36, 2024b.
- 693 Yuan Liu, Haodong Duan, Yuanhan Zhang, Bo Li, Songyang Zhang, Wangbo Zhao, Yike Yuan,
694 Jiaqi Wang, Conghui He, Ziwei Liu, et al. Mmbench: Is your multi-modal model an all-around
695 player? *arXiv preprint arXiv:2307.06281*, 2023c.

- 702 Yuan Liu, Le Tian, Xiao Zhou, and Jie Zhou. Rethinking overlooked aspects in vision-language
703 models. *arXiv preprint arXiv:2405.11850*, 2024c.
704
- 705 Yuliang Liu, Zhang Li, Biao Yang, Chunyuan Li, Xucheng Yin, Cheng-lin Liu, Lianwen Jin,
706 and Xiang Bai. On the hidden mystery of ocr in large multimodal models. *arXiv preprint*
707 *arXiv:2305.07895*, 2023d.
- 708 Haoyu Lu, Wen Liu, Bo Zhang, Bingxuan Wang, Kai Dong, Bo Liu, Jingxiang Sun, Tongzheng Ren,
709 Zhuoshu Li, Yaofeng Sun, et al. Deepseek-vl: towards real-world vision-language understanding.
710 *arXiv preprint arXiv:2403.05525*, 2024a.
711
- 712 Pan Lu, Ran Gong, Shibiao Jiang, Liang Qiu, Siyuan Huang, Xiaodan Liang, and Song-Chun Zhu.
713 Inter-gps: Interpretable geometry problem solving with formal language and symbolic reasoning.
714 In *The 59th Annual Meeting of the Association for Computational Linguistics (ACL)*, 2021a.
- 715 Pan Lu, Liang Qiu, Jiaqi Chen, Tony Xia, Yizhou Zhao, Wei Zhang, Zhou Yu, Xiaodan Liang,
716 and Song-Chun Zhu. Iconqa: A new benchmark for abstract diagram understanding and visual
717 language reasoning. *arXiv preprint arXiv:2110.13214*, 2021b.
718
- 719 Pan Lu, Swaroop Mishra, Tanglin Xia, Liang Qiu, Kai-Wei Chang, Song-Chun Zhu, Oyvind Tafjord,
720 Peter Clark, and Ashwin Kalyan. Learn to explain: Multimodal reasoning via thought chains for
721 science question answering. *Advances in Neural Information Processing Systems*, 35:2507–2521,
722 2022a.
- 723 Pan Lu, Liang Qiu, Kai-Wei Chang, Ying Nian Wu, Song-Chun Zhu, Tanmay Rajpurohit, Peter
724 Clark, and Ashwin Kalyan. Dynamic prompt learning via policy gradient for semi-structured
725 mathematical reasoning. *arXiv preprint arXiv:2209.14610*, 2022b.
726
- 727 Pan Lu, Hritik Bansal, Tony Xia, Jiacheng Liu, Chunyuan Li, Hannaneh Hajishirzi, Hao Cheng, Kai-
728 Wei Chang, Michel Galley, and Jianfeng Gao. Mathvista: Evaluating mathematical reasoning of
729 foundation models in visual contexts. *arXiv preprint arXiv:2310.02255*, 2023.
- 730 Shiyin Lu, Yang Li, Qing-Guo Chen, Zhao Xu, Weihua Luo, Kaifu Zhang, and Han-Jia Ye.
731 Ovis: Structural embedding alignment for multimodal large language model. *arXiv preprint*
732 *arXiv:2405.20797*, 2024b.
733
- 734 Max Marion, Ahmet Üstün, Luiza Pozzobon, Alex Wang, Marzieh Fadaee, and Sara Hooker.
735 When less is more: Investigating data pruning for pretraining llms at scale. *arXiv preprint*
736 *arXiv:2309.04564*, 2023.
- 737 Minesh Mathew, Dimosthenis Karatzas, and CV Jawahar. Docvqa: A dataset for vqa on document
738 images. In *Proceedings of the IEEE/CVF winter conference on applications of computer vision*,
739 pp. 2200–2209, 2021.
740
- 741 Minesh Mathew, Viraj Bagal, Rubèn Tito, Dimosthenis Karatzas, Ernest Valveny, and CV Jawahar.
742 Infographicvqa. In *Proceedings of the IEEE/CVF Winter Conference on Applications of Computer*
743 *Vision*, pp. 1697–1706, 2022.
- 744 Arindam Mitra, Hamed Khanpour, Corby Rosset, and Ahmed Awadallah. Orca-math: Unlocking
745 the potential of slms in grade school math, 2024.
746
- 747 OpenAI. Chatgpt, 2022. URL <https://openai.com/blog/chatgpt>.
- 748 OpenAI. Gpt-4 technical report. Technical Report 1, 2, 9, 10, OpenAI, 2023. URL <https://example.com/gpt4-technical-report>.
- 749
750
- 751 Baolin Peng, Chunyuan Li, Pengcheng He, Michel Galley, and Jianfeng Gao. Instruction tuning
752 with gpt-4. *arXiv preprint arXiv:2304.03277*, 2023.
753
- 754 Yuxuan Qiao, Haodong Duan, Xinyu Fang, Junming Yang, Lin Chen, Songyang Zhang, Jiaqi Wang,
755 Dahua Lin, and Kai Chen. Prism: A framework for decoupling and assessing the capabilities of
vlms. *arXiv preprint arXiv:2406.14544*, 2024.

- 756 Alec Radford, Jong Wook Kim, Chris Hallacy, Aditya Ramesh, Gabriel Goh, Sandhini Agarwal,
757 Girish Sastry, Amanda Askell, Pamela Mishkin, Jack Clark, et al. Learning transferable visual
758 models from natural language supervision. In *International conference on machine learning*, pp.
759 8748–8763. PMLR, 2021.
- 760 Naganand Yadati Sanket Shah, Anand Mishra and Partha Pratim Talukdar. Kvqa: Knowledge-aware
761 visual question answering. In *AAAI*, 2019.
- 762 Christoph Schuhmann, Romain Beaumont, Richard Vencu, Cade Gordon, Ross Wightman, Mehdi
763 Cherti, Theo Coombes, Aarush Katta, Clayton Mullis, Mitchell Wortsman, et al. Laion-5b: An
764 open large-scale dataset for training next generation image-text models. *Advances in Neural
765 Information Processing Systems*, 35:25278–25294, 2022.
- 766 Wenhao Shi, Zhiqiang Hu, Yi Bin, Junhua Liu, Yang Yang, See-Kiong Ng, Lidong Bing, and Roy
767 Ka-Wei Lee. Math-llava: Bootstrapping mathematical reasoning for multimodal large language
768 models. *arXiv preprint arXiv:2406.17294*, 2024.
- 769 Mohit Shridhar, Jesse Thomason, Daniel Gordon, Yonatan Bisk, Winson Han, Roozbeh Mottaghi,
770 Luke Zettlemoyer, and Dieter Fox. Alfred: A benchmark for interpreting grounded instructions
771 for everyday tasks. In *Proceedings of the IEEE/CVF conference on computer vision and pattern
772 recognition*, pp. 10740–10749, 2020.
- 773 Amanpreet Singh, Vivek Natarajan, Meet Shah, Yu Jiang, Xinlei Chen, Dhruv Batra, Devi Parikh,
774 and Marcus Rohrbach. Towards vqa models that can read. In *Proceedings of the IEEE/CVF
775 conference on computer vision and pattern recognition*, pp. 8317–8326, 2019.
- 776 Hui Su, Xiao Zhou, Houjin Yu, Xiaoyu Shen, Yuwen Chen, Zilin Zhu, Yang Yu, and Jie Zhou.
777 Welm: A well-read pre-trained language model for chinese. *arXiv preprint arXiv:2209.10372*,
778 2022.
- 779 Gemini Team, Rohan Anil, Sebastian Borgeaud, Yonghui Wu, Jean-Baptiste Alayrac, Jiahui Yu,
780 Radu Soricut, Johan Schalkwyk, Andrew M Dai, Anja Hauth, et al. Gemini: a family of highly
781 capable multimodal models. *arXiv preprint arXiv:2312.11805*, 2023.
- 782 Qwen Team. Qwen2.5: A party of foundation models, September 2024. URL [https://qwenlm.
783 github.io/blog/qwen2.5/](https://qwenlm.github.io/blog/qwen2.5/).
- 784 Teknium. Openhermes 2.5: An open dataset of synthetic data for generalist llm assistants, 2023.
785 URL <https://huggingface.co/datasets/teknium/OpenHermes-2.5>.
- 786 Shengbang Tong, Ellis Brown, Penghao Wu, Sanghyun Woo, Manoj Middepogu, Sai Charitha
787 Akula, Jihan Yang, Shusheng Yang, Adithya Iyer, Xichen Pan, et al. Cambrian-1: A fully open,
788 vision-centric exploration of multimodal llms. *arXiv preprint arXiv:2406.16860*, 2024.
- 789 Junke Wang, Lingchen Meng, Zejia Weng, Bo He, Zuxuan Wu, and Yu-Gang Jiang. To see is to
790 believe: Prompting gpt-4v for better visual instruction tuning. *arXiv preprint arXiv:2311.07574*,
791 2023.
- 792 Haoran Wei, Lingyu Kong, Jinyue Chen, Liang Zhao, Zheng Ge, Jinrong Yang, Jianjian Sun, Chun-
793 rui Han, and Xiangyu Zhang. Vary: Scaling up the vision vocabulary for large vision-language
794 models. *arXiv preprint arXiv:2312.06109*, 2023.
- 795 Mitchell Wortsman, Gabriel Ilharco, Samir Ya Gadre, Rebecca Roelofs, Raphael Gontijo-Lopes,
796 Ari S Morcos, Hongseok Namkoong, Ali Farhadi, Yair Carmon, Simon Kornblith, et al. Model
797 soups: averaging weights of multiple fine-tuned models improves accuracy without increasing
798 inference time. In *International conference on machine learning*, pp. 23965–23998. PMLR, 2022.
- 799 An Yang, Baosong Yang, Binyuan Hui, Bo Zheng, Bowen Yu, Chang Zhou, Chengpeng Li,
800 Chengyuan Li, Dayiheng Liu, Fei Huang, et al. Qwen2 technical report. *arXiv preprint
801 arXiv:2407.10671*, 2024.
- 802 Yuan Yao, Tianyu Yu, Ao Zhang, Chongyi Wang, Junbo Cui, Hongji Zhu, Tianchi Cai, Haoyu Li,
803 Weilin Zhao, Zhihui He, et al. Minicpm-v: A gpt-4v level mllm on your phone. *arXiv preprint
804 arXiv:2408.01800*, 2024.

- 810 Shukang Yin, Chaoyou Fu, Sirui Zhao, Ke Li, Xing Sun, Tong Xu, and Enhong Chen. A survey on
811 multimodal large language models. *arXiv preprint arXiv:2306.13549*, 2023.
812
- 813 Alex Young, Bei Chen, Chao Li, Chengen Huang, Ge Zhang, Guanwei Zhang, Heng Li, Jiangcheng
814 Zhu, Jianqun Chen, Jing Chang, et al. Yi: Open foundation models by 01. ai. *arXiv preprint*
815 *arXiv:2403.04652*, 2024.
- 816 Longhui Yu, Weisen Jiang, Han Shi, Jincheng Yu, Zhengying Liu, Yu Zhang, James T Kwok, Zhen-
817 guo Li, Adrian Weller, and Weiyang Liu. Metamath: Bootstrap your own mathematical questions
818 for large language models. *arXiv preprint arXiv:2309.12284*, 2023a.
819
- 820 Qiying Yu, Quan Sun, Xiaosong Zhang, Yufeng Cui, Fan Zhang, Yue Cao, Xinlong Wang, and
821 Jingjing Liu. Capsfusion: Rethinking image-text data at scale. In *Proceedings of the IEEE/CVF*
822 *Conference on Computer Vision and Pattern Recognition*, pp. 14022–14032, 2024.
- 823 Weihao Yu, Zhengyuan Yang, Linjie Li, Jianfeng Wang, Kevin Lin, Zicheng Liu, Xinchao Wang,
824 and Lijuan Wang. Mm-vet: Evaluating large multimodal models for integrated capabilities. *arXiv*
825 *preprint arXiv:2308.02490*, 2023b.
- 826 Ye Yuan, Xiao Liu, Wondimu Dikubab, Hui Liu, Zhilong Ji, Zhongqin Wu, and Xiang Bai.
827 Syntax-aware network for handwritten mathematical expression recognition. *arXiv preprint*
828 *arXiv:2203.01601*, 2022.
829
- 830 Xiang Yue, Xingwei Qu, Ge Zhang, Yao Fu, Wenhao Huang, Huan Sun, Yu Su, and Wenhao Chen.
831 Mammoth: Building math generalist models through hybrid instruction tuning. *arXiv preprint*
832 *arXiv:2309.05653*, 2023.
- 833 Xiang Yue, Yuansheng Ni, Kai Zhang, Tianyu Zheng, Ruoqi Liu, Ge Zhang, Samuel Stevens,
834 Dongfu Jiang, Weiming Ren, Yuxuan Sun, et al. Mmmu: A massive multi-discipline multi-
835 modal understanding and reasoning benchmark for expert agi. In *Proceedings of the IEEE/CVF*
836 *Conference on Computer Vision and Pattern Recognition*, pp. 9556–9567, 2024.
837
- 838 Pan Zhang, Xiaoyi Dong, Yuhang Zang, Yuhang Cao, Rui Qian, Lin Chen, Qipeng Guo, Haodong
839 Duan, Bin Wang, Linke Ouyang, et al. Internlm-xcomposer-2.5: A versatile large vision language
840 model supporting long-contextual input and output. *arXiv preprint arXiv:2407.03320*, 2024.
- 841 Peng Zhang, Can Li, Liang Qiao, Zhanzhan Cheng, Shiliang Pu, Yi Niu, and Fei Wu. Vsr: a unified
842 framework for document layout analysis combining vision, semantics and relations. In *Document*
843 *Analysis and Recognition–ICDAR 2021: 16th International Conference, Lausanne, Switzerland,*
844 *September 5–10, 2021, Proceedings, Part I 16*, pp. 115–130. Springer, 2021.
- 845 Yanzhe Zhang, Ruiyi Zhang, Jiuxiang Gu, Yufan Zhou, Nedim Lipka, Diyi Yang, and Tong Sun.
846 Llavar: Enhanced visual instruction tuning for text-rich image understanding. *arXiv preprint*
847 *arXiv:2306.17107*, 2023.
- 848 Chunting Zhou, Pengfei Liu, Puxin Xu, Srinivasan Iyer, Jiao Sun, Yuning Mao, Xuezhe Ma, Avia
849 Efrat, Ping Yu, Lili Yu, et al. Lima: Less is more for alignment. *Advances in Neural Information*
850 *Processing Systems*, 36, 2024.
851
- 852 Deyao Zhu, Jun Chen, Xiaoqian Shen, Xiang Li, and Mohamed Elhoseiny. Minigpt-4: En-
853 hancing vision-language understanding with advanced large language models. *arXiv preprint*
854 *arXiv:2304.10592*, 2023.
855

856 A VISUAL INSTRUCTION TUNING DATASETS

857
858 Table 6 shows the visual instruction tuning datasets used in this work.
859

860 B PROMPT FOR CAPFUSION

861
862 Figure 4 shows the prompts to generate new image caption and merge the original caption and the
863 generated caption.

Category	Dataset
Conversation	LLaVAR(Zhang et al., 2023), inhouse GPT-4o data, Mini-Gemini(Li et al., 2024b) LVIS-Instruct4V(Wang et al., 2023)
Document	DocVQA(en)(Mathew et al., 2021)
Caption	ALLaVA(Chen et al., 2024a), ShareGPT4V(Chen et al., 2023), LAION-GPT4V
General QA	VSR(Zhang et al., 2021), IConQA(Lu et al., 2021b)
Science	AI2D(Kembhavi et al., 2016), TQA(Kim et al., 2018), ScienceQA(Lu et al., 2022a)
Chart&Screen	DVQA(Kafle et al., 2018), POIE(Kuang et al., 2023), MapQA (Chang et al., 2022) ScreenQA (Hsiao et al., 2022)
Mathematics	GeoQA+(Cao & Xiao, 2022), Geo3K(Lu et al., 2021a), TabMWP(Lu et al., 2022b) CLEVR-Math(Lindström & Abraham, 2022), SuperCLEVER(Li et al., 2023b), MathV360K (Shi et al., 2024)
Knowledge	KVQA(Sanket Shah & Talukdar, 2019)
OCR	InfoVQA(Mathew et al., 2022), TextVQA(Singh et al., 2019) ST-VQA(Biten et al., 2019), ICDAR2015, HME100K(Yuan et al., 2022)
Text-only	LIMA(Zhou et al., 2024), Alpaca-GPT4(Peng et al., 2023) OpenHermes2.5(Teknium, 2023), MetaMathQA(Yu et al., 2023a) MathInstruct(Yue et al., 2023), orca-math-word-problems-200k(Mitra et al., 2024) atlas-math-sets, Math

Table 6: Visual instruction tuning datasets to build the strong baseline and the those finally selected to conduct model soup (marked in red).

Generate Image Caption

<ImageHere>Please briefly describe the image in English

Fuse Original Caption and Generated Image Caption

The following two sentences are different descriptions of the same picture, please merge and refine the information in the two given sentences.

Sentence 1 provides detailed world knowledge, but there are defects in sentence structure and grammar. Sentence 2 shows good sentence structure, but lacks in-depth real-world details and may contain erroneous information.

Please merge them into a new sentence, ensuring good sentence structure while retaining the detailed real-world information provided in sentence 1. There are several requirements:

1. Please organically combine the descriptions of the two sentences about the picture, without any traces of adhesion.
2. At the same time, do not introduce any information that has not appeared in these two sentences.
3. Please only return the merged sentence, do not provide other information.

Sentence 1: {original caption}
Sentence 2: {generated image caption}
Merged Sentence:

Figure 4: Prompt for image caption generation and captions merging.

C PROMPT FOR INHOUSE GPT-4O DATASET

Figure 5 shows the prompt to generate the inhouse GPT-4o data in Table 6.

918
919
920
921
922
923
924
925
926
927
928
929
930
931
932
933
934
935
936
937
938
939
940
941
942
943
944
945
946
947
948
949
950
951
952
953
954
955
956
957
958
959
960
961
962
963
964
965
966
967
968
969
970
971

```

## Generate inhouse GPT-4o Dataset
You are an AI visual assistant, please ask two questions about the content of the image and give the
corresponding answer.
Requirements:
1. The question need complex reasoning to be answered.
2. The answer can be obtained confidently
3. Provide detailed answers when answering complex questions. For example, give detailed examples
or reasoning steps to make the content more convincing and well-organize
4. The perspective of asking questions needs to be more diverse, and at the same time, the sentence
structure of the questions also needs to be more varied.
5. Please give question&answer pairs in the following format with no serial number:
<question>
<answer>
    
```

Figure 5: Prompt to generate the inhouse GPT-4o dataset.

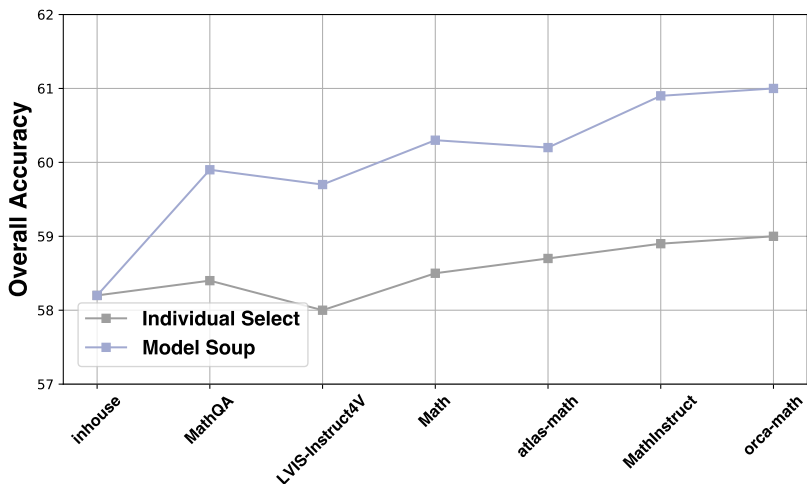


Figure 6: Model Soup brings consistent improvement regardless of what Base Set is used.

D MODEL SOUP WITH DIFFERENT BASE SET

To verify that model soup consistently improves performance regardless of the Base Set used, we randomly sampled 6 datasets from the Base Set in Table 6 to conduct model soup, while the remaining datasets were used as the new Base Set. As shown in Figure 6, model soup also brings significant improvements compared to individual selection, demonstrating the effectiveness and universality of model soup.

E HOMOGENEITY IN EXISTING PRE-TRAINING DATASET

We randomly sampled 5 million images from LAION-5B and used POINTS to identify the main object in each image. We then plotted the distribution of the top six objects from the sampled data. As shown on the left side of Figure 7, these six objects account for more than 90% of the total data. The right side of Figure 7 illustrates the distribution of the top six objects after applying a simple balancing technique: if the count of a particular object exceeds the average count of the top six objects, we down-sample it to 60% of its total count. We re-trained the strong baseline model on both the original and balanced pre-training datasets. The overall score of the balanced version outperformed the original by 0.6. This is an initial investigation into the distribution of the pre-training dataset, and we plan to explore this direction further in our future research.

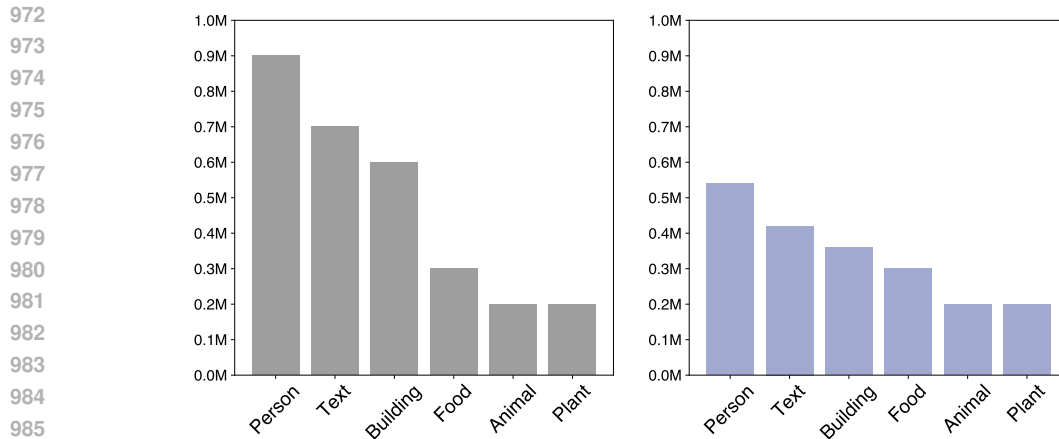


Figure 7: Top 6 objects from the subset we randomly sample from LAION-5B (left), and the distribution of the top 6 objects after simple balance (right).

F CASE STUDY OF PRE-TRAINING DATASET

As discussed in Section 3.2, we filter the pre-training dataset using perplexity. Figure 8 shows samples randomly selected from the top 20% and bottom 20% of the data, which have the lowest perplexity values. As illustrated, the captions in the bottom 20% of the data are more likely to contain obscure world knowledge. While augmenting the model with more world knowledge during pre-training can help it generalize better in real-world scenarios, the relatively small scale of the vision-language model pre-training dataset makes this obscure world knowledge in the bottom 20% quite sparse (seldom appearing more than once during pre-training). Consequently, this world knowledge is more likely to be noise rather than informative content for pre-training. Additionally, we also use InternVL2 (Chen et al., 2024d) to filter the pre-training dataset. The model pre-trained on the filtered subset achieves an overall score of **60.1**, surpassing the model pre-trained on the original 5M dataset by **1.1** points.

G ABLATION ABOUT THE MAXIMUM NUMBER OF TILES

We perform more fine-grained ablation studies about the maximum number of tiles used in CATTY, and Figure 9 shows the results.

H ABLATION ABOUT THE FEATURE AVERAGE FROM VISION ENCODER

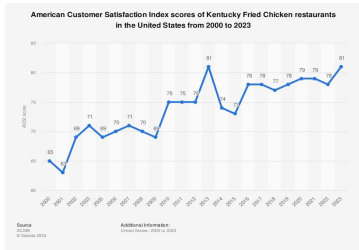
Before feeding features into the LLM, we compute the weighted average of features from both the general and OCR vision encoders. Figure 10 illustrates the model’s performance when different weights are assigned to the general vision encoder (note that the weights assigned to the general and OCR vision encoders sum to 1). In this ablation study, we adhere to the experimental settings described in the fifth row of Table 1 in the main paper.

I TRAINING COST OF POINTS

We employ data parallelism (DP) (Li et al., 2020) to distribute the data and tensor parallelism (TP) (Shridhar et al., 2020) to partition the model across multiple GPUs. All our models are trained using $32 \times$ H800 80G GPUs. The pre-training stage is completed in 3 hours, while the visual instruction tuning stage takes 7 hours.

1026
1027
1028
1029
1030
1031
1032
1033
1034
1035
1036
1037
1038
1039
1040
1041
1042
1043
1044
1045
1046
1047
1048
1049
1050
1051
1052
1053
1054
1055
1056
1057
1058
1059
1060
1061
1062
1063
1064
1065
1066
1067
1068
1069
1070
1071
1072
1073
1074
1075
1076
1077
1078
1079

Top 20%



The provided line graph visually illustrates the American Customer Satisfaction Index scores of Kentucky Fried Chicken restaurants across the United States, from the year 2000 up to 2023.



The diligent businesswoman, clad in a professional attire, steadfastly ascends the staircase, symbolizing her unwavering pursuit of goals. She carries her briefcase, embodying her dedication and commitment to her work. Each step she takes represents a strategic move towards achieving her objectives, showcasing her resilience and determination in the face of challenges.



This image displays a pair of sarcophagi from Tutankhamen's tomb in the Valley of the Kings. The first sarcophagus is unadorned, while the second one is intricately crafted and engraved with gold, showcasing the pharaoh's intricate mummy wrappings. These sarcophagi represent the opulence and prestige of ancient Egyptian royalty and provide valuable insights into their burial customs and beliefs.

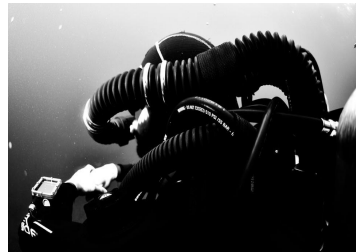


Olivia Palermo, a well-known fashion influencer, showcases her style versatility in two contrasting photos. In one, she sports a casual outfit with a comfortable, yet stylish, pair of Aquazzura shoes. In the other, she elegantly dons a more formal ensemble, making a statement with her fashion-forward choices.

Last 20%



The **2-Pack Natali Grommet Top Curtain Panels** with Details showcase a refined aesthetic, featuring black curtains elegantly draped over a gold rod, creating a sophisticated and stylish ambiance in any room.



Valéry PLATON's Shark Rebreathers Photos exhibit a striking black and white image of a diver's equipment.



The **Attraction Dice Online Slot Demo Game**, showcased on a graphic with three dice and the words "Dice Attraction" in front of a blue background, is provided by **GAMING1**.



The **Antic Wood Door at Fort**, as seen in Video Clip **#72616182 on Pond5**, is an old and weathered doorway featuring a wooden door and stone columns.

Figure 8: The left are samples randomly selected from the top 20% and the right are samples randomly selected from the last 20%. These obscure world knowledge is marked in red.

1080
1081
1082
1083
1084
1085
1086
1087
1088
1089
1090
1091
1092
1093
1094
1095
1096
1097
1098
1099
1100
1101
1102
1103
1104
1105
1106
1107
1108
1109
1110
1111
1112
1113
1114
1115
1116
1117
1118
1119
1120
1121
1122
1123
1124
1125
1126
1127
1128
1129
1130
1131
1132
1133

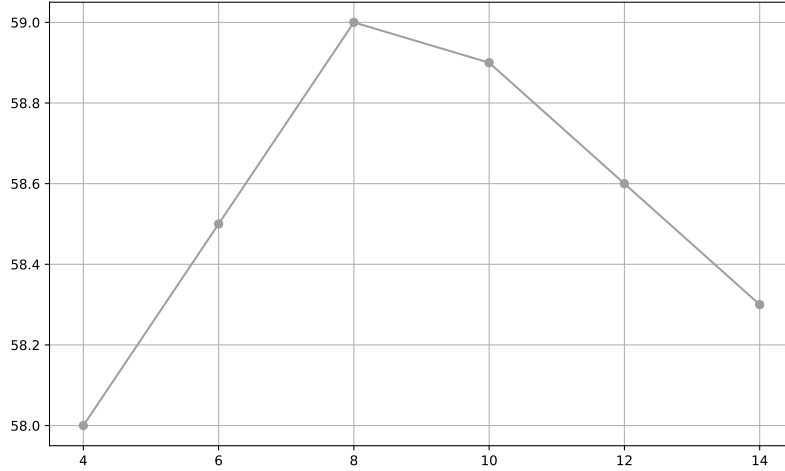


Figure 9: Ablation study about the maximum split used in CATTY.

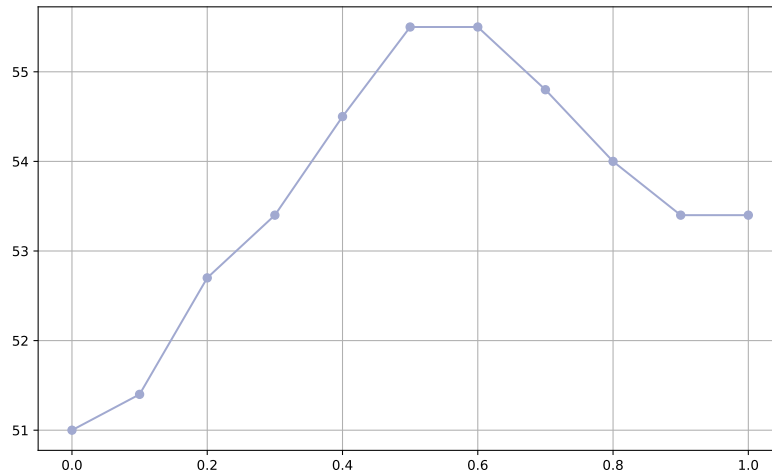


Figure 10: Ablation about the weight assigned to the general vision encoder.